

Fracture properties of concrete exposure to delayed ettringite formation

C. Rocco & F. Giangrasso

Facultad de Ingeniería, Universidad Nacional de La Plata, Argentina.

L. Bergol, G. Di Pace

Centro Técnico Loma Negra, Argentina

J. Planas

E.T.S.I. Caminos, Canales y Puertos, Universidad Politécnica de Madrid, España.

ABSTRACT: The effect of damage produced by delayed ettringite formation, DEF, on the fracture properties of concrete are evaluated experimentally using the cohesive crack model framework. Five concretes containing cements with different composition were studied. All concretes were submitted to Fu's accelerated curing method to trigger DEF, stored under water at 23 ± 1 °C during 180 days and then tested. Both stable three-point bend test, according to RILEM recommendation, and splitting test were performed. From these tests the specific fracture energy, splitting tensile strength and bilinear softening curve were obtained. Additionally, longitudinal resonance frequency and length change were recorded during the curing time. The results show that the fracture mechanics parameters proved to be an adequate tool to measure concrete deterioration due to "DEF". As the DEF in the matrix increased, the evolution of the softening curve shown that the maximum cohesive tensile stress decreases whereas the critical opening crack increases. As consequence of these changes the fracture energy remains constant and the concrete becomes more "ductile".

Keywords: concrete, durability, delayed ettringite, fracture properties, cohesive crack model.

1. INTRODUCTION

Ettringite formation is considered to be the cause of most of the expansion and disruption of concrete structures involved in sulfate attack (ACI Committee 201, 1994). However, not necessarily any ettringite formation produces damage in concrete. When ettringite formation occurs early in the plastic concrete state, for instance, when the gypsum and the anhydrous calcium aluminate present in the cement react during the first minutes, it does not cause any disruptive action. Moreover, ettringite formation is useful to control the setting time of concrete. This type of ettringite formation is known as early ettringite formation (EEF). On the other hand, when ettringite forms in the hardened concrete state, after several days, months or years, the non-uniform expansion associated with its formation can produce cracking and spalling in the concrete. This type of ettringite is known as delayed ettringite formation (DEF),

(Diamond 1996, Fu & Beauvoisin 1996a, Collepardi 1999, Taylor et al. 2001).

Depending on the sulfate source, there are two different types of DEF (Collepardi 2003). One is due to the typically known external sulfate attack (ESA), which occurs when permeable concretes are in contact with water or soils containing sulfate ions. The other is due to internal sulfate attack (ISA), which occurs in a sulfate-free environment when the sulfate source is inside the concrete. This relatively "new" mechanism of DEF, detected in the 1980s in prestressed concrete railway ties (Mielenz et al. 1995), fundamentally occurs when the early ettringite formation produced in the plastic concrete state is decomposed by thermal action and re-forms later in the hardened concrete state. The thermal source to destroy early ettringite can be external, as occurs in concrete exposure to steam curing above 70°C, or internal, as can occur in mass concrete due to the heat released during the early hydration process (Heinz & Ludwig 1987, Glasser 1996, Odler & Chen 1996, Yang et al. 1999).

Recently, many experimental studies have been conducted to evaluate the influence of concrete composition and exposure conditions upon the DEF due to ISA (Lawrence 1995, Older & Chen 1995, Kelham 1996, Zhang et al. 2002a). Most of these studies have focused on the parameters that govern ettringite formation and the expansion that it produces, especially on the effect of the cement composition and on the thermal history during concrete curing. Nevertheless, it is surprising to note that although the ISA can produce serious damage in concrete structures, less attention has been paid to evaluate how the cracking and microcracking induced by ISA can affect both the fracture and mechanical properties of concrete.

In this work, experimental results are presented to show the effect of delayed ettringite formation on the fracture parameters of concrete. To induce delayed ettringite formation the studied concretes were elaborated using cements with appropriate sulfate contents, exposed to elevated temperature at an early age and then stored under water for 180 days. During this period both the expansion history and the dynamic modulus of elasticity were recorded. At 180 days, the fracture parameters of concretes were determined experimentally. The macroscopic fracture parameters were characterized by means of the cohesive crack model, which has shown its usefulness in modeling the fracture process in concrete and concrete-like materials. Using the cohesive crack model as a framework, the effect of induced concrete damage by DEF on the tensile strength, f_t , specific fracture energy, G_F , elastic modulus of elasticity, E , and on the softening curve is shown. To develop different levels of damage in the concrete, five batches with different cement compositions were studied.

A brief description of the cohesive crack model concepts is presented in the following section. The materials and specimens used in this study, and the tests performed are presented in Section 3. The experimental results and discussion are given in Section 4. On the basis of the obtained results, the main conclusions are presented in Section 5.

2. FRACTURE CHARACTERIZATION

To characterize the fracture parameters of concrete, the cohesive crack model framework was used. This is one of the models which best describes the nonlinear fracture processes in concrete-like materials. The model introduces the softening

function to simulate the microcracking and deterioration of the material in the fracture process zone, which is modeled by means of a cohesive crack, which can transfer stress from one face to the other. The softening function relates the cohesive stress transferred between the crack faces to the crack opening in each point of the fracture surface, and is considered to be a material property.

The maximum stress in the cohesive crack is equal to the tensile strength of the material, f_t , and decreases progressively as the crack opening increases. When the crack opening reaches the critical crack opening, w_c , the cohesive stress drops to zero and a true – stress-free – crack propagates. The work done to produce a true crack unit area is the specific fracture energy, G_F , and coincides with the area under the softening curve. The fracture energy, the tensile strength, the critical crack opening and the softening function itself are all macroscopic material properties, and thus are dependent on the internal microstructure of concrete. The cohesive crack concepts are shown schematically in Figure 1.

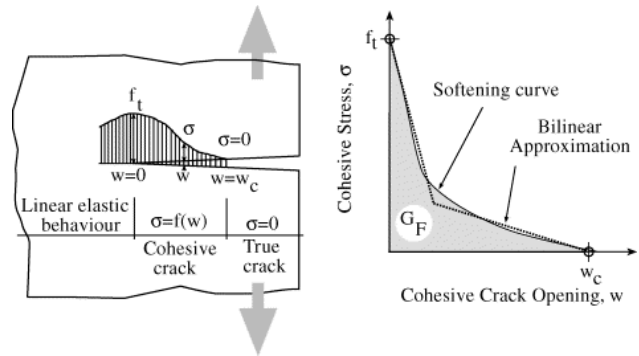


Figure 1. Cohesive crack and softening function

A parameter directly related to the cohesive zone extension, during the fracture process, is the characteristic length, l_{ch} , defined by Hillerborg et al. 1976, as:

$$l_{ch} = \frac{EG_F}{f_t^2} \quad (1)$$

This parameter is commonly used to characterize the brittleness of concrete. The smaller the l_{ch} value the more brittle the material is.

In this work, the softening function was approximated by a four-parameter bilinear function. As many authors have pointed out, this simple

diagram suffices to describe the fracture behavior of concrete. To determine the four parameters necessary to fit the bilinear softening function, the general bilinear fit method proposed by Guinea et al. 1994 was used, and stable three-point bending tests on notched beams and Brazilian splitting tests were conducted.

3. MATERIALS AND TESTS

1.1 Materials and Specimens

Cement: two commercially available portland cements, ordinary portland cement, OPC similar to ASTM Type I, and high sulfate resistant cement, HSRC, similar to ASTM Type V, were used as primary cements. To modify both the sulfate and alumina content in cement, gypsum (G) and a commercial sulfate-aluminate-based powder additive, free of calcium oxide, ONODA (O), were employed. So, two unmodified portland cement types, OPC and HSRC, and three modified sulfate portland cement types, OPC+G, OPC+O and HSRC+G, were used to elaborate the concretes.

Table 1 shows the principal components of cement, expressed as percent by weight of cement, in relation to the DEF. In the same table, the SO_3/Al_2O_3 ratio and the DEF index, as proposed by Zhang et al. 2002b, are included.

Table 1. Cement composition

| Component | Type of cement | | | | |
|-------------------------------------------------|----------------|-------|-------|------|--------|
| | OPC | OPC+G | OPC+O | HSRC | HSRC+G |
| SO ₃ , % | 2.86 | 4.17 | 4.04 | 1.90 | 3.92 |
| C3A, % | 8.14 | 7.90 | 7.71 | 0.99 | 0.90 |
| Na ₂ O _{eq} , % | 1.42 | 1.36 | 1.26 | 0.70 | 0.57 |
| Al ₂ O ₃ , % | 5.32 | 5.16 | 5.01 | 3.56 | 3.43 |
| SO ₃ /Al ₂ O ₃ | 0.54 | 0.81 | 0.81 | 0.53 | 1.14 |
| DEF index | 0.71 | 1.14 | 1.07 | 0.13 | 0.41 |

Aggregate: the coarse aggregate was crushed granite with nominal sizes between 6 and 20 mm, and a fineness modulus of 6.54. Two different fine aggregates were used and both were natural siliceous sands with a fineness modulus of 3.16 and 1.82 respectively.

Concrete mix: five batch concretes of similar potential strength at 28 day were elaborated using the cement types indicated in table 1. All concrete batches were similar, with a cement content of 380 kg/m³, a water-cement ratio, w/c, of 0.45 and a slump (ASTM C 143) of 100 ± 20 mm. In order to

obtain the same slump and the same w/c ratio for all mixes, a medium range plasticizer, based on lignosulfonate (Pozzolith 322-N from MBT), at an appropriate proportion was used. The concrete batches were identified in accordance with the cement used.

Specimens: for each concrete batch, four prismatic specimens of 100 x 75 x 400 mm³ for fracture property determinations and three prismatic specimens of 100 x 100 x 250 mm³ for change in length measurements were cast. Then, the specimens were treated as described below.

1.2 Curing treatment

To trigger Delayed Ettringite Formation the specimens were subjected to the curing cycles proposed by Fu 1996b. After casting, the specimens were left at 23°C for one hour and then placed in a steam-curing chamber until they reached 95°C in one hour, and were maintained at 95°C for 12 hours. Temperature was then dropped to 23°C in 4 hours. The specimens were then immersed in water for 6 hours and afterward placed in an oven at 85°C for 24 hours. Finally, and after cooling at room temperature, the specimens were immersed in limewater at 23 ± 1°C up to testing age at 180 days. This curing cycle causes sulfate absorption by the hydrated calcium silicate, C-S-H, gel during steam curing, then the microcracking of concrete during thermal drying and finally the slow release of sulfate from C-S-H gel, its migration into cracks and the reaction with aluminum-bearing components of the cement matrix during water curing (Fu & Beaudoin 1996c)

1.3 Tests performed for fracture properties

Two sets of experiments were carried out to characterize the fracture properties of each concrete batch: stable three-point bend fracture test and Brazilian splitting test. The three-point bend test on quarter-notched beams was performed following the RILEM TC 50 recommendations, enhanced with some additional suggestions by Guinea et al. 1992, Planas et al. 1992 and Elices et al. 1992. Beams of 100 mm depth were tested in bending, with a span-to-depth ratio of 3.65. During the test, load-point displacement and crack mouth opening displacement were continuously recorded. The Brazilian splitting test was conducted on 100 x 100 x 75 mm square section prismatic specimens cut from the broken halves of bending tests. The splitting test was conducted according to ASTM

C496 except for the size of the specimen and width of the load-bearing strips, which was equal to 8 mm — 8% of the specimen depth — as recommend by Rocco et. al. 1999a. For each concrete batch, four bending specimens and five Brazilian splitting specimens were tested, all at 180 days.

From the tests mentioned above, the fracture energy, G_F , the tensile strength, f_t , the critical crack opening, w_c , and the shape of the bilinear softening curve were determined by the general fit method proposed by Guinea et al. 1994, and are shown in the next section.

Additionally, periodical determinations of both change in length, performed according to ASTM C 490 on 100 x 100 x 250 mm prismatic specimens, and longitudinal resonance frequency to dynamic modulus of elasticity determinations, according to ASTM C 215-97 on 100 x 75 x 400 mm prismatic specimens, were recorded during the specimen curing time until the time of the fracture tests.

4. RESULTS AND DISCUSSION

In the following subsections the experimental results are presented and discussed.

1.4 Change in length and dynamic modulus of elasticity history

Figure 2 shows the expansion history of each concrete during the curing period and the final change in length at 180 days. As can be noted, the final expansion at 180 days is in accordance with the DEF index indicated in table 1. As the DEF index increases, the change in length also increases for the same time. This expansion behavior is associated with the quantity of delayed ettringite formed in the concrete matrix, which depends mainly on the SO_3 and Al_2O_3 content, and on the SO_3 / Al_2O_3 ratio.

As can be seen in figure 2, the concretes with significant ettringite development, batch OPC+G and OPC+O, as well as a higher final expansion level, show an increased expansion rate and an asymptotic final behavior. On the other hand, HSRC concrete, which has the lowest DEF index, exhibits a very slow expansion development with a very low final expansion level. OPC and HRS+G concretes show an intermediate behavior.

Figure 3 shows the evolution of the dynamic modulus of elasticity of concretes during the curing period. Note that in HSRC concrete, which does not show expansive behavior, the dynamic modulus

practically remains constant after 30 days. This behavior is typical of unaltered concretes. On the other hand, the four concretes that experienced expansion by delayed ettringite formation show a significant reduction in dynamic modulus after 30 days. In these concretes, the dynamic modulus of elasticity decreases monotonically up to a same threshold value, and the ratio as the modulus drops is proportional to the expansion ratio. From both the change in length and dynamic modulus values we can estimate that the dynamic modulus threshold value was reached when the concrete expansion was between 0.3 and 0.5%. It is possible that this expansion level marks the beginning of severe cracking in the concrete.

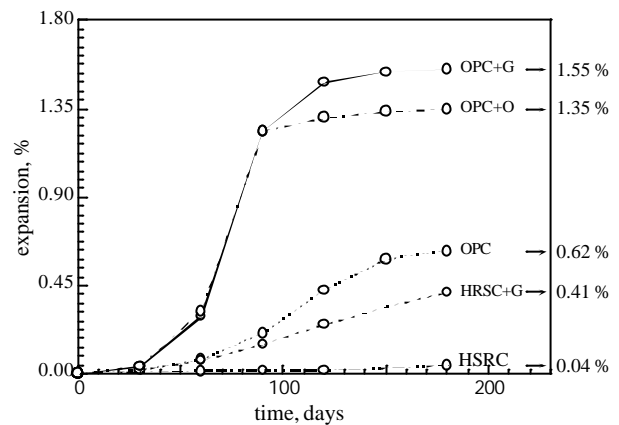


Figure 2. Expansion – time plots

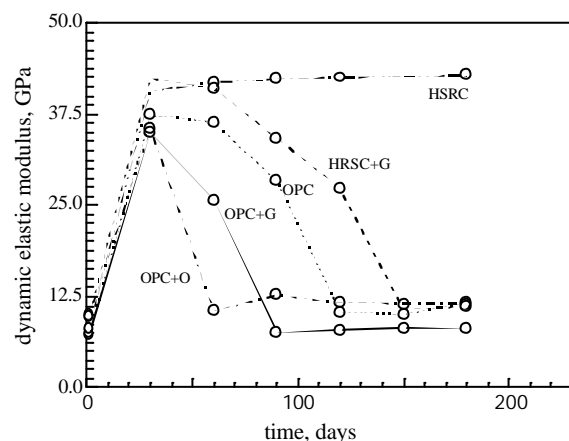


Figure 3. Dynamic modulus of elasticity – time plots

The reduction in the dynamic modulus of elasticity is a consequence of the cracking and micro-

cracking induced in the cementitious matrix of concrete by the effect of the expansion produced during ettringite formation. The presence of cracking, on the surface of expansive concrete specimens, was visually verified

1.5 Tensile strength, modulus of elasticity and fracture energy

The mean values of the tensile strength, f_t , static modulus of elasticity, E_s and fracture energy, G_F , experimentally determined at 180 days are given in table 2. The values correspond to mean test values.

The static modulus of elasticity was determined from the load-cmod compliance measured in the three-point bend test. The characteristic length, l_{ch} , calculated according to expression (1) is included in the same table.

Table 2: Properties of concrete

| Material Property | Concrete | | | | |
|--------------------------------------------|----------|-------|-------|------|--------|
| | OPC | OPC+G | OPC+O | HSRC | HSRC+G |
| Tensile strength, f_t (in MPa) | 1.75 | 1.13 | 1.26 | 2.85 | 1.90 |
| Modulus of elasticity, E_s (in GPa) | 10.3 | 6.3 | 8.6 | 31.0 | 11.3 |
| Fracture energy, G_F (in N/m) | 166 | 136 | 144 | 124 | 169 |
| Characteristic length, l_{ch} (in mm) | 461 | 677 | 780 | 474 | 501 |

Figures 4 to 7 show the material properties, included in table 2, in terms of the expansion level in the concrete at the time these properties were determined – 180 days. The error bars that correspond to the range of variation of experimental results and the fitting curves obtained from the experimental mean values are also indicated in the figures.

As can be inferred from figures 4 and 5, the microcracking produced in the concrete due to expansion affect the concrete tensile strength, f_t , and the modulus of elasticity, E_s . Note that the higher the developed expansion level in the concrete is, as a consequence of the DEF, the lower both the tensile strength and the modulus of elasticity are. For the concretes tested in these cases, the decrease in tensile strength and modulus of elasticity, in the concrete with higher expansion levels, was up to 60% and 80% respectively.

With respect to fracture energy, G_F , as shown in Figure 6, no significant changes were observed.

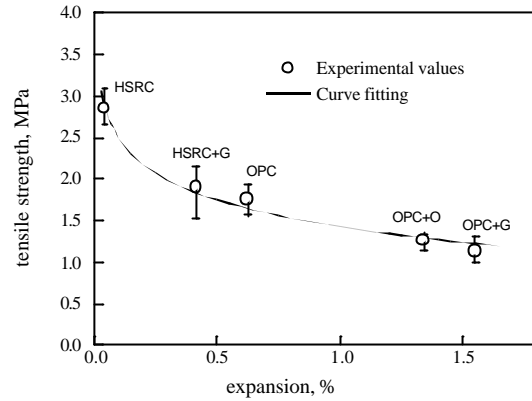


Figure 4. Tensile strength of the different concretes in terms of the expansion level at 180 day.

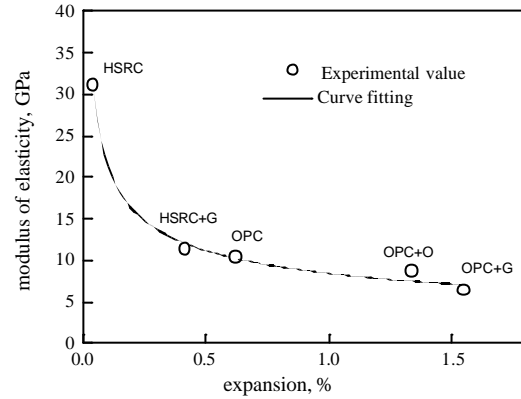


Figure 5. Static modulus of elasticity of the different concretes in terms of the expansion level at 180 day

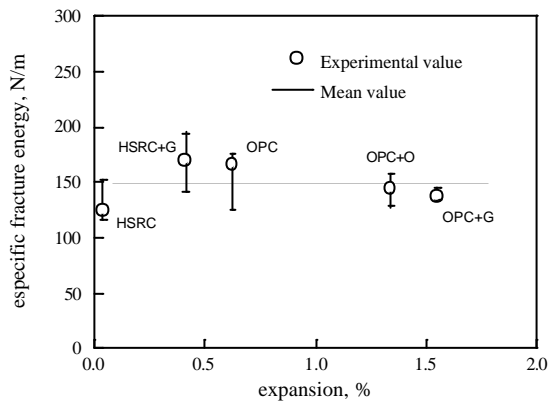


Figure 6. Specific fracture energy of the different concretes in terms of the expansion level at 180 day

Irrespective of the expansion level, the individual values of G_F , remain in the same range with extreme values between 120 and 200 N/m, and a mean value of 150 N/m.

Figure 7 shows the characteristic length, l_{ch} , of concretes. As can be seen, concretes with an expansion level up to 0.6% have similar values of l_{ch} , with mean values close to 500 mm. Nevertheless, an increment in the characteristic length was observed in the concretes with an expansion level higher than 1.2%. In this case, the values of l_{ch} increased up to 800 mm indicating a change in the concrete brittleness.

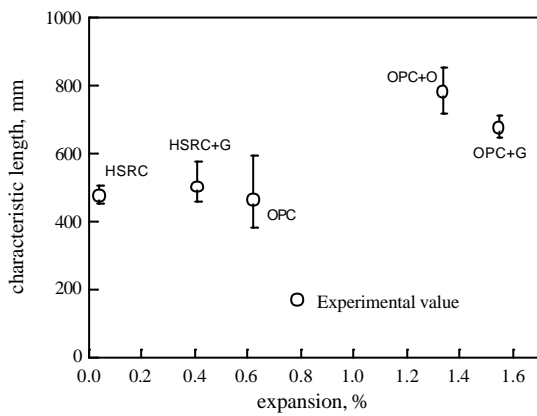


Figure 7. Characteristic length of the different concretes in terms of our expansion level at 180 day

1.6 Softening curves

Figures 8 and 9 plot the representative softening function, determined at 180 days, for each one of the five concretes studied. These curves, summarized as the fracture properties of concrete, are affected by the damage induced by delayed ettringite formation. As can be seen, the expansion level of the concrete, and the associated damage, meaningfully affect the parameters of the softening function, particularly the tensile strength (as mentioned above) and the critical crack opening. As the level of expansion increases, the concrete softening curves display a larger critical crack opening and a lower tensile strength. For the studied concrete and the resulting expansion ranges, a practically linear variation of the critical crack opening with the expansion level was observed. This tendency can be seen in Figure 10, where the relation between critical crack opening and expansion is shown.

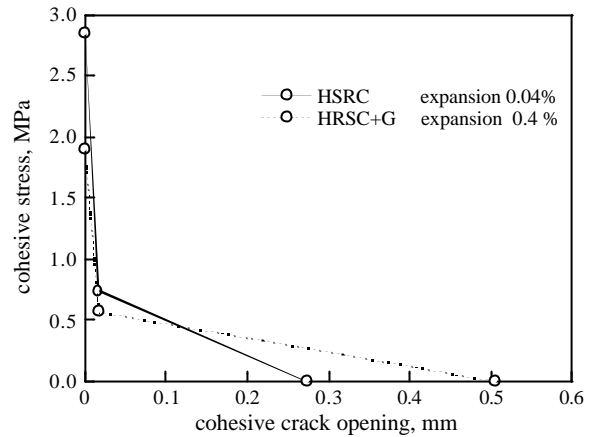


Figure 8. Softening curves for concretes with an expansion level lower than 0.5%.

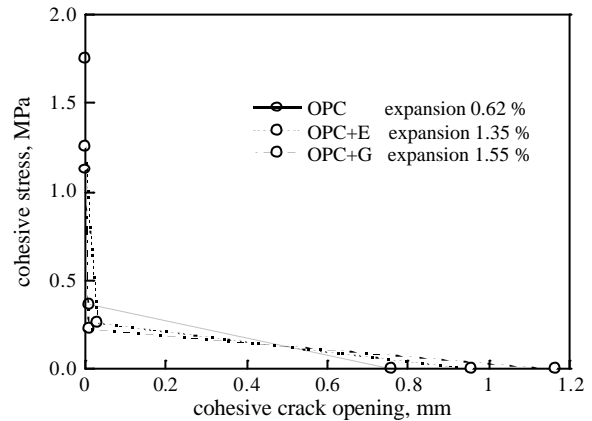


Figure 9. Softening curves for concretes with an expansion level higher than 0.5%.

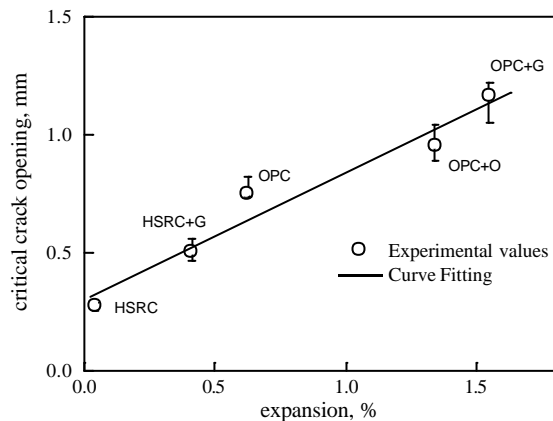


Figure 10. Variation in critical crack opening with the expansion level at 180 days

The enlargement in the tail softening curve imparts to the concrete a higher stress transference capability in the fracture process zone. The reason for this behavior can be related to the change in the aggregate interlocking and overlapping crack mechanisms as a consequence of the microcracking induced in the concrete during delayed ettringite formation. Nevertheless, this assumption has to be tested with further research

With respect to the break point in the bilinear softening curve, we have only observed changes in the cohesive tensile stress break point value. The way in which this value varies with the expansion can be seen in figure 11. Note that as the expansion increases the cohesive tensile stress corresponding to the break point in the softening curve decreases.

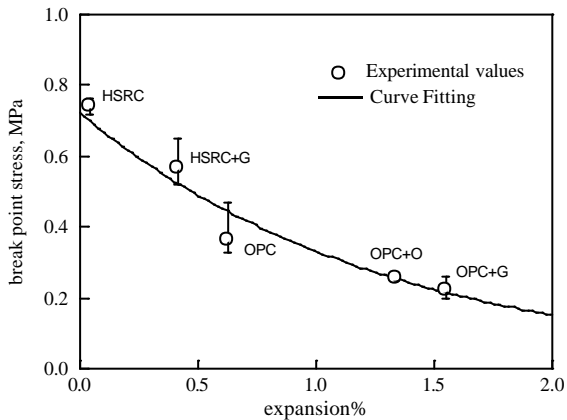


Figure 11. Variation in cohesive stress on the break point softening curve with the expansion level at 180 days.

5. CONCLUSIONS

This experimental work shows the influence of the microcracking-induced damage, due to delayed ettringite formation, DEF, on the fracture and elastic properties of concrete. The conclusions to be drawn from this study can be summarized as follows:

- During the beginning of the DEF process, the dynamic modulus of elasticity of concrete decreases progressively as the expansion advances. However, an asymptotic nonzero threshold value, close to 10 GPa, was observed when the expansion was between 0.3% and 0.4%. It seems that when the microcracking induced by the expansion

achieves a certain level, the resonance frequency method used to evaluate the dynamic modulus becomes insensitive. The relation between the threshold dynamic modulus value and the induced damage in concrete is worth investigated further.

- Both the modulus of elasticity and tensile strength of concrete are strongly affected by the micro-cracking induced by DEF. For an expansion level of 1.56% a drop up to 80% in the static elastic modulus, and 60% in the tensile strength were measured in this work.

- Non appreciable change on the specific fracture energy, G_F , were measured due to the induced damage in concrete by ettringite formation. With independence of the expansion level reached, G_F remained practically constant in all studied concretes.

- For expansion level higher than 1,2% (high cracking development) an increment in the characteristic length was observed. As a consequence concrete becomes more “ductile”.

- Microcracking induced by DEF, affects appreciably the concrete softening curve. As the damage increase, the maximum cohesive tensile stress, f_t , that the material can transferred in the fracture process zone decrease, whereas that the critical opening crack, w_c , increase. These parameters showed a very closed correlation with the change of length produced in the concrete during the DEF.

6. ACKNOWLEDGEMENTS

The authors gratefully acknowledge Loma Negra Technical Center for the design, casting and curing of the concrete used in this work, and for the determination of the dynamic modulus and change in length during the curing period. They are also grateful to the Aeronautic Department of the National University of La Plata for supplying the testing machine used in the fracture bending test.

J. Planas and C. Rocco, then acknowledge to the Ramon y Cajal Program and the support provided by the Spanish Comisión Interministerial de Ciencia y Tecnología (CICYT) under grants MAT 2001-3863-C03-01

7. REFERENCES

- ACI Committee 201. 1994. Guide to durable concrete. ACI manual of concrete practice Part 1. Detroit.
- Collepari., M. 1999. Damage by delayed ettringite formation. *Concrete International*, 21 (1): 69-74.
- Collepari. 2003. A state-of-the-art review on delayed ettringite attack on concrete. *Cement & Concrete Composites*, 25 : 401-407.
- Diamond, S. 1996. Delayed ettringite formation-process and problems. *Cement & Concrete Composites*, 18: 243-256.
- Elices, M. Guinea, G. & Planas, J. 1992. Measurement of the fracture energy using three point bend tests: 3. Influence of cutting the P- δ tail. *Materials & Structures*, 25: 327-334.
- Fu, Y & Beauidoin, J. 1996a. Mechanism of delayed ettringite formation in Portland cement system. *ACI Material journal*. 327-333.
- Fu, Y. 1996b. Delayed Ettringite Formation in Portland Cement Products. PhD Thesis, University of Ottawa, Canada.
- Fu, Y & Beauidoin, J. 1996c. Microcracking as a precursor to delayed ettringite formation in cement systems. *Cement and Concrete Research*, 26 (10): 1493-1498.
- Glasser, F. 1996. The role of sulfate mineralogy and cure temperature in delayed ettringite formation. *Cement & Concrete Composite*, 18 (3) : 187-193.
- Guinea, G. Planas, J & Elices, M. 1992. Measurement of the fracture energy using three point bend tests: 1. Influence of experimental procedures. *Materials & Structures*, 25: 212-218.
- Guinea, G. Planas, J & Elices, M. 1994. A general bilinear fit for the softening curve of concrete. *Materials & Structures*, 27: 99-105.
- Heinz, U. & Ludwig, U. 1987. Mechanims of secondary ettringite formation in mortars and concretes subjected to heat treatment. In Scanlon, J. (ed), *SP 100 american Concrete Institute, Detroit*, vol. 2: 2059-2071.
- Hillerborg, A. Mod er, P. & Petersson, P. 1976. analysis of crack formation and crack growth in concrete by means of fracture mechanics and finite elements. *Cement and Concrete Research*, 6: 773-782.
- Kelham, S. 1996. The effect of cement composition and fineness on expansion associated with delayed ettringite formation. *Cement & Concrete Composite*, 18: 171-179.
- Lawrence, C. 1995. Mortar expansion due to delayed ettingite formation. Effect of curing period and temperature. *Cement and Concrete Research*, 25 (4): 903-914.
- Mielenz, R., Marusin, S. Hime, W. & Judovic, Z. 1995. Investigation of prestressed concrete railway tie distress. *Concrete International*, 17 (12): 62-68.
- Odler, I & Chen, Y. 1995. Effect of cement composition on the expansion of heat-cured cement pastes. *Cement and Concrete Research*, 25 (4): 853-862.
- Odler, I & Chen, Y. 1996. On the delayed expansion of heat cured Portland cement pastes and concretes. *Cement & Concrete Composite*, 18: 181-185.
- Planas, J. Elices, M. & Guinea, G. 1992. Measurement of the fracture energy using three point bend tests: 2. Influence of bulk energy dissipation. *Materials & Structures*, 25: 305-312.
- RILEM TC 50 FCM. 1985. Draft Recommendation. Determination of the fracture energy of mortar and concrete by means of three-point bend test on notched beams. *Materials & Structures*, 18 (106): 285-290.
- Rocco, C., Guinea, G. Planas, J. & Elices, M. 1999a. Size effect and boundary conditions in the Brazilian test: Experimental verification. *Materials & Structures*, 32: 210-217.
- Rocco, C., Guinea, G. Planas, J. & Elices, M. 1999b. Size effect and boundary conditions in the Brazilian test: Theoretical analysis. *Materials & Structures*, 32: 437-444.
- Taylor, H., Famy, C. & Scrivener, K. 2001. Delayed ettringite formation, Review. *Cement and Concrete Research.*, 31: 683-693.
- Yang, R. Lawrence, C. Lynslade, C. & Sharp, J. 1999. Delayed ettringite formation in heat-cured Portland cement mortars. *Cement and Concrete Research*, 29 (1): 17-25.
- Zhang, Z. Olek, J. & Diamond, S. 2002a. Studies on delayed ettringite formation in early age heat cured mortars I. Expansion measurements, changes in dynamic modulus of elasticity, and weight gains. *Cement and Concrete Research*, 32: 1729-1736.
- Zhang, Z. Olek, J. & Diamond, S. 2002b. Studies on delayed ettringite formation in heat-cured mortars II. Characteristic of cement that may be susceptible to DEF. *Cement and Concrete Research*, 32: 1737-1742.